AIP Advances

Ga-, Y-, and Sc-substituted M-type ferrites for self-biasing circulators in LTCC microwave modules

Cite as: AIP Advances **10**, 025315 (2020); https://doi.org/10.1063/1.5130419
Submitted: 18 October 2019 . Accepted: 13 January 2020 . Published Online: 11 February 2020

Manuel Heidenreich, Xinyi Ma, Wanja Gitzel, Arne Jacob, Beate Capraro, and Jörg Töpfer

Ga-, Y-, and Sc-substituted M-type ferrites for self-biasing circulators in LTCC microwave modules

Cite as: AIP Advances 10, 025315 (2020); doi: 10.1063/1.5130419
Presented: 5 November 2019 • Submitted: 18 October 2019 •
Accepted: 13 January 2020 • Published Online: 11 February 2020

Manuel Heidenreich,[1] Xinyi Ma,[1] Wanja Gitzel,[2] Arne Jacob,[2] Beate Capraro,[3] and Jörg Töpfer[1,a)]

AFFILIATIONS

[1] Ernst-Abbe-Hochschule Jena, 07745 Jena, Germany
[2] Hamburg University of Technology, 21073 Hamburg, Germany
[3] Fraunhofer IKTS, 07629 Hermsdorf, Germany

Note: This paper was presented at the 64th Annual Conference on Magnetism and Magnetic Materials.
[a)] **Corresponding author**: Prof. Dr. J. Töpfer, Ernst-Abbe-Hochschule Jena, University of Applied Sciences Jena, C.-Zeiss-Promenade 2, 07745 JENA, GERMANY, **Tel.:** +49 3641 205479, **Fax**: +49 3641 205451, **E-Mail**: joerg.toepfer@eah-jena.de

ABSTRACT

The partial substitution of Fe^{3+} by diamagnetic Me^{3+} in $BaMe_xFe_{12-x}O_{19}$ with Me = Ga and Y ($0 \le x \le 2$) was studied. Samples were synthesized by the mixed-oxide route and their properties were compared to $BaSc_xFe_{12-x}O_{19}$ ferrites. It was shown by XRD that the hexagonal lattice parameters with x for Me = Ga and Sc vary continuously. For Me = Y no single-phase ferrites were obtained indicating that the solubility limit for Y in Ba ferrite is very limited. For Me = Ga and Sc, the saturation magnetization at room temperature is reduced with x. The coercivity as well as the ferromagnetic resonance frequency remain almost unchanged for Ga-substituted ferrites, whereas for Sc-substituted ferrites the coercivity and ferromagnetic resonance frequency decrease with x. Thick films of Sc-ferrite (x = 0.5) were screen-printed onto LTCC tape substrates and post-fired at 900°C. Application of a magnetic field during drying allows fabrication of textured ferrite layers. Alternatively, ferrite tapes and LTCC tapes were successfully co-fired at 900°C.

I. INTRODUCTION

Future satellite communication technologies require microwave ferrites capable of being integrated in LTCC multilayer modules for operation at high frequency, e.g. within the Ka-band (26-40 GHz). Substituted hexagonal M-type ferrites $BaMe_xFe_{12-x}O_{19}$ exhibit significant potential as self-biasing microwave components, such as isolators and circulators.[1–3] Microwave communication devices require magnetic materials with resonance frequencies in the operational frequency range. Spinel ferrites and garnets have rather low resonance frequencies. Their resonance peaks can be shifted to higher frequencies through use of bulky biasing magnets. Hexagonal ferrites, on the other hand, exhibit ferromagnetic resonances (FMR) at microwave and millimeter wave bands. In addition, they provide sufficient remanent magnetization and anisotropy to allow self-biasing. Consequently, no additional bias magnets are needed in microwave systems, opening opportunities for miniaturization and integration.[1–3] Hexagonal ferrite thick[4] and thin films[5] have already been proposed for magnetic microwave components.

The crystal structure of the M-type hexagonal ferrite (space group $P6_3/mmc$) may be described by a stacking of R- and S-blocks with sequence SRS∗R∗ (∗ denotes a 180° rotation around the c-axis). The Fe^{3+} ions occupy five different crystallographic sites: 12***k*** octahedral sites between R- and S-blocks, tetrahedral $4f_{IV}$ (or f_1) sites in the S-blocks, octahedral $4f_{VI}$ (or f_2) sites in the R-blocks, bipyramidal 2***b*** sites in the R-blocks, and octahedral 2***a*** sites in S-blocks. The magnetic moments on the 12***k***, 2***b*** and 2***a*** sites are parallel to the c-axis, whereas the magnetic moments on $4f_{IV}$ and $4f_{VI}$ sites are oriented antiparallel to the c-axis, resulting in a

ferrimagnetic arrangement with a total magnetic moment of 20 μ_B per formula unit.[6] $BaFe_{12}O_{19}$ has a magneto-crystalline anisotropy constant of $K_1 = 10^6$ erg/cm^3 with a corresponding anisotropy field of 17 kOe.[6,7] It was shown for single crystals that the ferromagnetic resonance (FMR) appears at 46 GHz, increasing with an applied static field.[8] Substitution of Fe^{3+} ions by diamagnetic cations such as Al^{3+}, In^{3+}, Ga^{3+} or Sc^{3+} has proven to be an effective way of tailoring the microwave properties of M-type ferrites. Substitution of Al increases H_a and FMR,[9] whereas they are reduced upon Sc- or In-substitution.[9–11] Moreover, at Sc-concentrations of about x = 1.8 the anisotropy was shown to change from uniaxial to planar,[9] this transition was shown to be strongly temperature dependent.[12] Ga-substitution $BaGa_xFe_{12-x}O_{19}$ has also been reported for the substitution range of $0 \le x \le 2$. In this case, the anisotropy field was shown to be nearly independent on composition x.[9] Trukhanov *et al.*[13] reported similar results with resonance behavior in the range of 46 – 48 GHz. Recently, Y-substitution was reported to be possible up to about x = 0.3.[14] However, experimental data on Ga- and Y-substitution in M-type ferrite are scarce and contradictory, hence a systematic study on phase formation and magnetic properties of Ga- and Y- substituted hexagonal ferrites is highly desired.

The integration of polycrystalline, oriented ferrite films into multilayer structures fabricated by the low-temperature ceramic co-firing (LTCC) technology, is another challenging topic. Complex electronic microwave devices, e.g. satellite communication modules, are fabricated using LTCC technology. Substituted M-type hexagonal ferrites with their FMR in the desired frequency band and self-biasing ability exhibit significant potential for miniaturization of such microwave devices. Integration of hexagonal microwave ferrites into LTCC multilayer architectures has not been documented yet. Recently, the fabrication of anisotropic ferrite layers by screen-printing onto alumina substrates and firing at 900°C has been demonstrated. Ferrite particle orientation and film anisotropy was induced by drying the printed ferrite films in a magnetic field.[15]

Here, we report on the synthesis, sintering behavior and magnetic properties of substituted $BaMe_xFe_{12-x}O_{19}$ M-type ferrites with Me = Ga and Y ($0 \le x \le 2$) and compare them with their Sc-substituted counterparts. We also report for the first time on co-firing and post-firing of ferrite layers with low-dielectric LTCC tapes at 900°C. This demonstrates the potential of oriented hexagonal ferrite layers as embedded magnetic components in LTCC microwave modules operating at K-band frequencies.

II. EXPERIMENTAL

Samples of $BaMe_xFe_{12-x}O_{19}$ (Me = Ga and Y) with x = 0, 0.25, 0.5, 0.75, 1.0, 1.25, 1.50, 1.75 and 2.0 were prepared by mixing Fe_2O_3, $BaCO_3$ and Ga_2O_3 or Y_2O_3 in stoichiometric proportions. After wet mixing of the starting materials, the powder mixture was calcined for 4 hours at 1300 °C for Ga-substituted, and at 1000-1300 °C for Y-substituted samples, respectively. The calcined powders were wet milled with ZrO_2 grinding media in a Fritzsch Pulverisette 6 planetary ball mill. For low-temperature sintering a mixture of 3 wt% of Bi-B-Si-Zn glass (BBSZ) powder and 2 wt% CuO was added during milling. Pellets were fabricated by uniaxial pressing. Ga-substituted ferrites were sintered for 4 hours at 1400 °C.

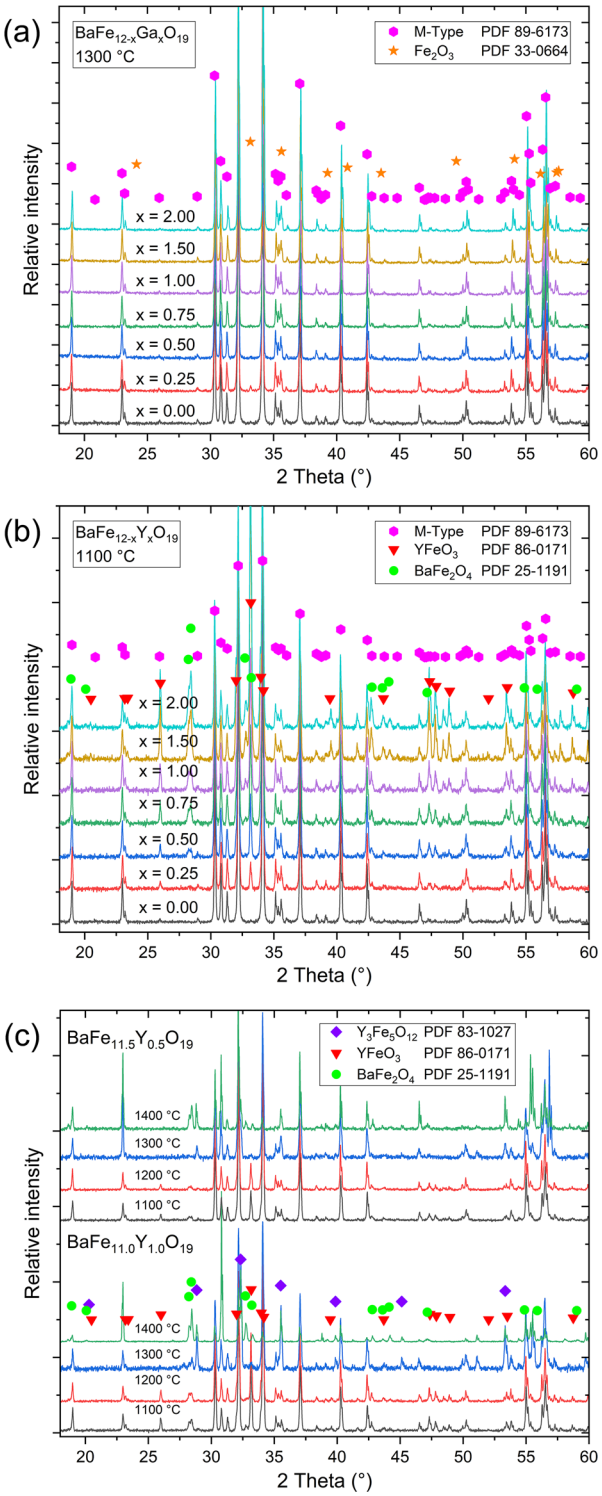

FIG. 1. X-ray diffraction patterns of $BaGa_xFe_{12-x}O_{19}$ ferrites with $0 \le x \le 2$ calcined at 1300 °C (a), of $BaY_xFe_{12-x}O_{19}$ ferrites with $0 \le x \le 2$ calcined at 1100 °C (b), and of $BaY_xFe_{12-x}O_{19}$ ferrites with x= 0.5 and x = 1.0 calcined at 1100 °C, 1200 °C, 1300 °C and 1400 °C (c).

A ferrite paste was prepared by mixing ferrite powder $BaSc_{0.5}Fe_{11.5}O_{19}$ with terpineol and cellulose binders. The paste was screen-printed onto CT708 LTCC tapes which were already pre-fired at 2 hours at 900 °C. The printed films were dried at 160 °C for 2 hours in a static magnetic field of H = 6 kOe which was applied perpendicular to the film direction. The magnetic field was generated by two SmCo permanent magnets. The printed films were positioned in the airgap between the magnets placed in the oven. After drying, the films were heated to 500 °C with 0.5 K/min for binder burnout, and then to 900 °C with 4 K/min and sintered at 900 °C for 2 hours. A ferrite tape with 100 μm thickness was prepared by tape casting. Two ferrite tape layers were stacked between two CT708 LTCC layers on top and bottom and laminated. The whole multilayer stack was co-fired at 900 °C for 2 hours.

X-ray patterns were recorded with a Bruker AXS D8 Advance diffractometer using Cu K_α radiation. Lattice parameters were obtained through Rietveld refinements using Bruker Topas 6 software. The powder particle size was measured using laser diffraction (Malvern Mastersizer 2000) and the specific surface of the powder was measured by nitrogen adsorption (BET, Nova 2000, Quantachrome Instruments). Shrinkage measurements were made on cylindrical compacts with a Netzsch DIL402 dilatometer with 4 K/min heating rate. The bulk density of sintered samples was determined with Archimedes' method. The microstructure of the sintered ferrites was investigated using an Ultra 55 Field Emission Scanning Electron Microscope (Zeiss). The microstructural anisotropy of the printed ferrite films was characterized by measuring pole figures (Bruker D8 Discover diffractometer) of the (006), (107) and ($1\bar{2}4$) lattice planes with a tilt angle Psi χ = 0 - 78° (increment $\Delta\chi$ = 3°) in a full circle Phi ϕ = 0 - 360° (increment $\Delta\phi$ = various). The pole figures were calculated using Bruker Texture 4.1; further data evaluation and plotting was performed using the MTEX toolbox 5.1.1[16] for MATLAB (The MathWorks Inc., Natick, USA). Hysteresis loops were measured at room temperature on powdered samples using a VSM magnetometer (MicroMag TM 3900, Princeton Measurements Corp., USA). The ferromagnetic resonant frequency was determined by return loss measurements in short-circuited waveguides. The sintered material was cut into thin rectangular bars which were placed in front of the short circuit. The measurements were performed with an Agilent PNA E8361A network analyzer in three frequency bands using WR-42 (18-26.5 GHz), WR-28 (26.5-40 GHz), and WR-19 (40-60 GHz) rectangular waveguides. No external magnetic field was applied during the measurements.

III. RESULTS AND DISCUSSION

Samples of $BaGa_xFe_{12-x}O_{19}$ with $0 \le x \le 2$ were calcined at 1300 °C. A single M-type ferrite phase is formed after calcination as confirmed through X-ray diffraction patterns (Fig. 1a). Powders of $BaY_xFe_{12-x}O_{19}$ with $0 \le x \le 2$ were calcined at different temperatures between 1100 to 1400 °C. The XRD patterns of samples calcined at 1100°C revealed that a ferrite phase has formed (Fig. 1b). However, it was found for that for all compositions the ferrite is in equilibrium with $YFeO_3$ and $BaFe_2O_4$ as additional phases. Even for the lowest substitution rate of x = 0.25 we did not obtain pure Y-substituted hexagonal ferrite. The phase composition was also studied for different calcination temperatures. As examples, we show the results for compositions x = 0.5 and x = 1.0 in Fig. 1c. At 1100 °C and 1200 °C, the formation of $YFeO_3$ and $BaFe_2O_4$ next to the ferrite main phase is observed. At T ≥ 1300 °C $Y_3Fe_5O_{12}$ and $BaFe_2O_4$ form as secondary phases besides ferrite. However, for all compositions x and at all temperatures studied, we did not observe a Y-substituted ferrite single phase. This is in contrast to the results of Chen *et al.*,[14] who claim that a small ferrite solid solution range exists for x ≤ 0.3. Our experiments reveal, that no solid solution range $BaY_xFe_{12-x}O_{19}$ seems to exist, and/or the solubility limit of Y in Ba ferrite is extremely small. Further experiments with Y-substituted multi-phase samples were not performed.

Hexagonal lattice parameters a_0 and c_0 of $BaGa_xFe_{12-x}O_{19}$ were obtained from refinements of XRD powder patterns in space group $P6_3/mmc$ (No. 194). The unit cell parameters are shown as function

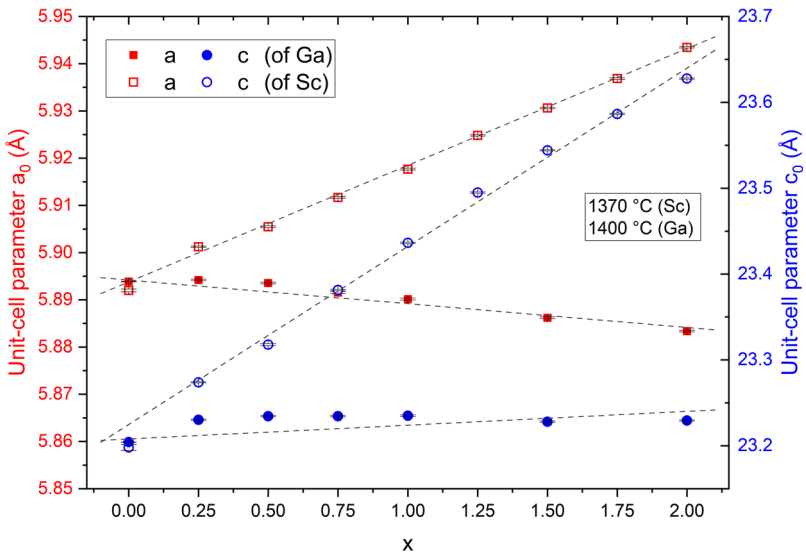

FIG. 2. Variation of hexagonal unit cell parameters vs. substitution rate x for $BaGa_xFe_{12-x}O_{19}$ (filled symbols) and $BaSc_xFe_{12-x}O_{19}$ (open symbols, data from[11]).

of Ga-concentrations in Fig. 2; data for $BaSc_xFe_{12-x}O_{19}$ are included for comparison. A slight decrease of a_0 and increase of c_0 is found for Ga-substituted ferrites. This is different from the results in Ref. 13, where a significant decrease of c_0 from x = 0 to x = 1.2 was reported.

For Sc-substituted ferrites, a linear increase of the unit cell dimensions was observed.[11] This observed expansion of the unit cell can be explained by the larger ionic radius of Sc^{3+} (0.745 Å) and the smaller one for Ga^{3+} (0.62 Å) as compared to Fe^{3+} (0.645 Å).[17] Since Sc^{3+}

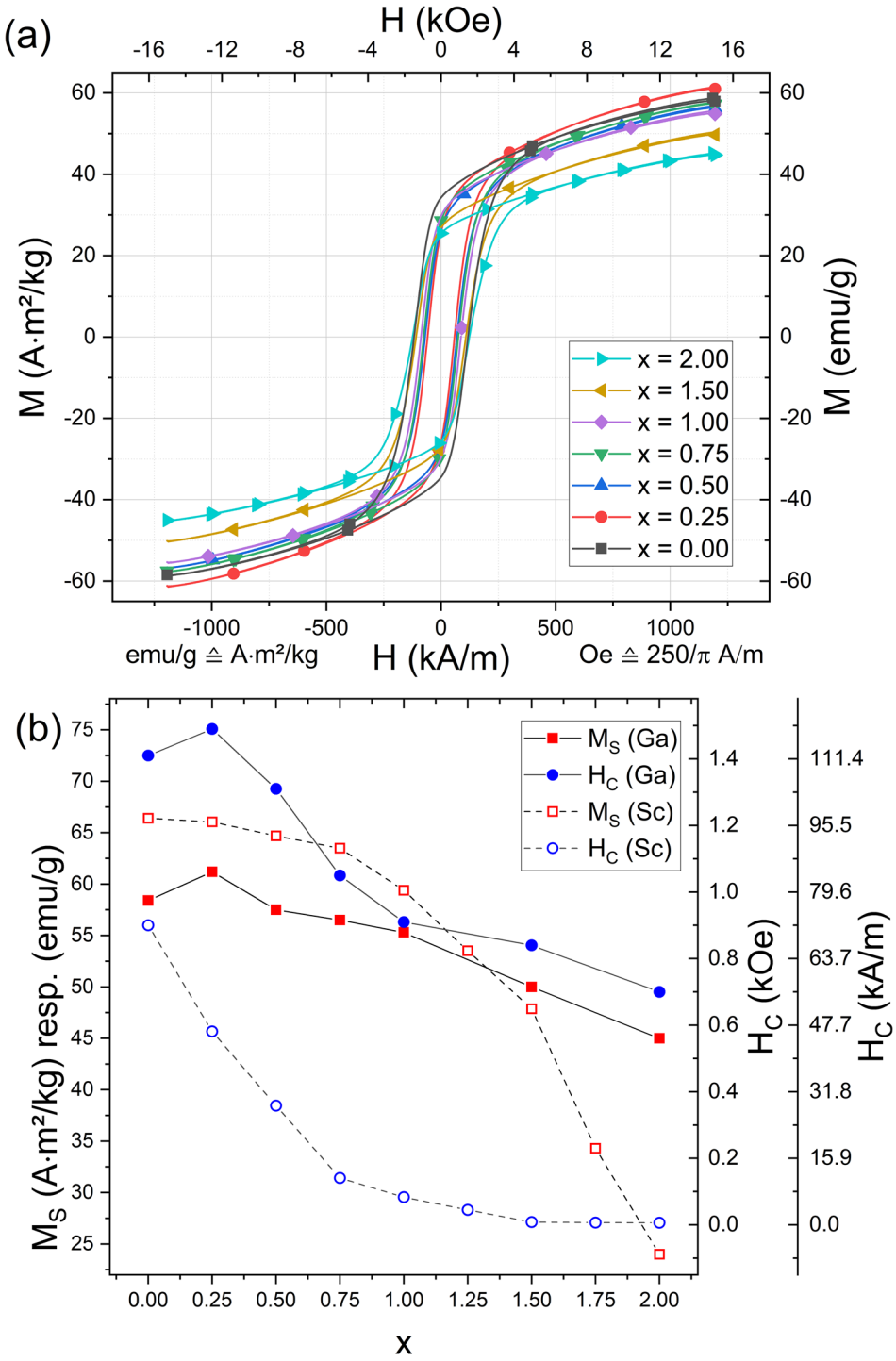

FIG. 3. Room-temperature hysteresis loops of $BaFe_{12-x}Ga_xO_{19}$ ferrites with $0 \leq x \leq 2$ (a) and variation of the saturation magnetization and coercive field at room temperature for $BaGa_xFe_{12-x}O_{19}$ (filled symbols) and $BaSc_xFe_{12-x}O_{19}$ (open symbols, data from[11]) as function of x (b).

ions were shown to prefer occupation of R-block octahedral $4f_{vi}$ and five-fold $2b$ sites,[18] the partial occupation of these sites by large Sc^{3+} ions leads to a expansion of the unit cell in a- and c-directions. In the case of Ga, the slightly smaller ionic size gives rise to small shrinkage of the unit cell. In contrast to that, substitution of large Ln^{3+} cations on Ba^{2+} sites (which are part of the hexagonal oxygen packing) leads to a shrinkage of the unit cell in c-direction, as shown e.g. for $Sr_{1-x}La_xFe_{12}O_{19}$.[19]

The calcined powders were fine milled to a particle size of about d_{50} = 2 μm, the specific surface area was about 5 m^2/g. Pellets of $BaGa_xFe_{12-x}O_{19}$ were sintered at 1400 °C for 4 hours. The resulting density of the sintered samples are in the range of 96% to 98%. In order to reduce the sintering temperature, a mixture of BBSZ and CuO was added as liquid phase sintering aid. The temperature of maximum shrinkage rate (as observed by dilatometry) is reduced down to T_{MSR} = 800 °C (not shown here). Samples sintered for 4 hours at 900 °C reach densities of 91% - 94%. This indicates that substituted M-type ferrites can be co-fired at low temperatures around 900°C with LTCC materials, and hence are compatible with requirements of LTCC technology.

Room temperature hysteresis loops for $BaGa_xFe_{12-x}O_{19}$ are shown in Fig. 3a. BaM ferrite (x = 0) with uniaxial anisotropy exhibits a broad M-H loop. As the Ga-concentration increases, the saturation magnetization as well as the coercivity slightly decrease. For both, Ga- and Sc-substituted ferrites, M_s is reduced starting from about 57-69 emu/g at x = 0. In the Ga-substituted ferrites, M_s is moderately decreased to 45 emu/g at x = 2, whereas for Sc-substitution Ms is decreased to 25 emu/g at x = 2,[11] respectively (Fig. 3b). The coercivity is slightly reduced only from H_c = 1.4 kOe for x = 0 to H_c = 0.7 kOe for x = 2 in the Ga-substituted ferrites (Fig. 3b). For Sc-substituted ferrites, on the other hand, a dramatic drop of coercivity down to a few Oe at x = 2 was found.[11] The observed reduction of M_s is caused by the replacement of Fe^{3+} ions with a magnetic moment of 5 μ_B by nonmagnetic Me^{3+} ions. Based on the Gorter ferrimagnetic model of co-linear spin arrangements, Ba ferrite has a saturation magnetization of 20 μ_B (105 emu/g) at 4 K which is reduced to about 70 emu/g at room temperature.[6,7] Sc^{3+} cations have a clear preference for R-block octahedral $4f_{vi}$ and five-fold $2b$ sites, as shown by Mössbauer spectroscopy.[18,20] Up to x = 2, the substitution of non-magnetic ions on 12k sites is negligible.[18] Since $4f_{vi}$ sites contribute to the spin-down sublattice, replacement of ferric by nonmagnetic ions would increase the total magnetic moment. Gorters model, assuming antiparallel spin arrangements, does not allow to interpret the observed reduction of M_s with x. On the other hand, one may expect, that the presence of diamagnetic ions on $4f_{vi}$ sites disturbs the super-exchange coupling with ferric ions on $12k$ sites; therefore the orientations of the magnetic moments of such 12k iron ions in the neighborhood of Sc^{3+}or Ga^{3+} ions deviate from the z-axis. This is confirmed by the observation of two 12k sextets in the Mössbauer spectra.[18] Accordingly, significant spin canting is expected to appear with increasing substitution level x, reducing the net magnetization for larger Sc/Ga concentrations. The decrease of coercivity with x (Fig. 3b) is attributed to a reduction in the uniaxial magneto-crystalline anisotropy. This is consistent with the results of Röschmann *et al.*,[9] who showed that the anisotropy field in $BaGa_xFe_{12-x}O_{19}$ is at around 17 kOe for all compositions, whereas in the case of $BaSc_xFe_{12-x}O_{19}$ H_a decreases from 17 kOe for

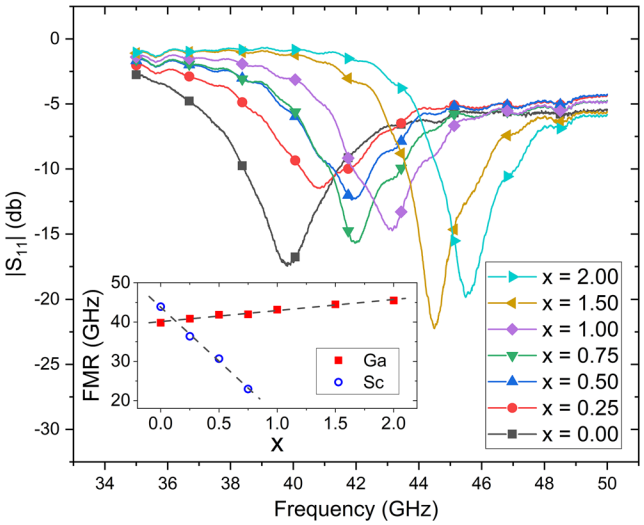

FIG. 4. Magnitude of the reflection coefficient vs. frequency of $BaFe_{12-x}Ga_xO_{19}$ with $0 \le x \le 2$ sintered at 1400 °C, inset: variation of the resonance frequency for $BaGa_xFe_{12-x}O_{19}$ (filled symbols) and $BaSc_xFe_{12-x}O_{19}$ (open symbols, data from[11]) as function of x.

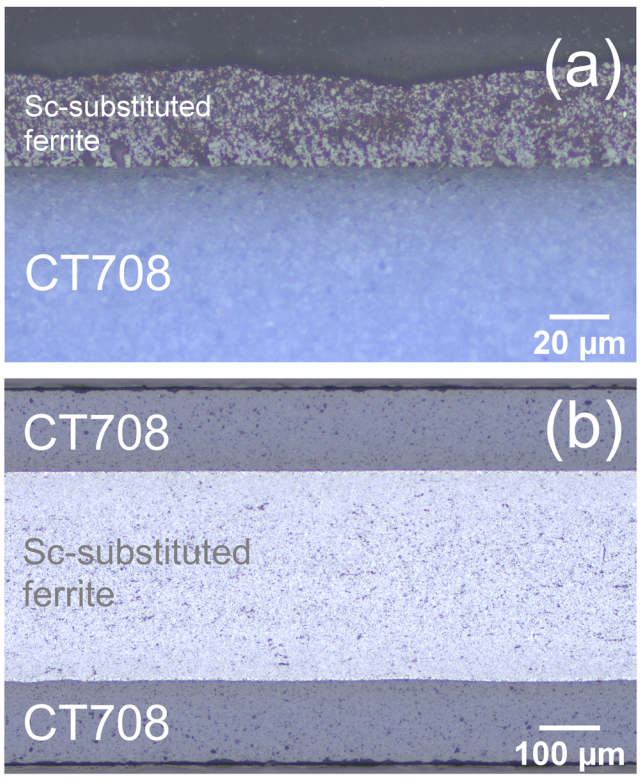

FIG. 5. Microscopy micrograph (cross-section) of a textured film of $BaSc_{0.5}Fe_{11.5}O_{19}$ printed onto a LTCC substrate and post-fired at 900 °C (a), and of a multilayer stack of $BaSc_{0.5}Fe_{11.5}O_{19}$ layers embedded in CT708 LTCC layers and co-fired at 900 °C (b).

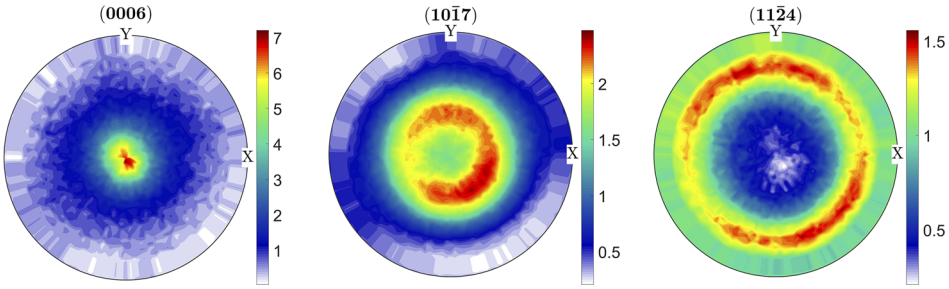

FIG. 6. XRD pole figures of (006), (107) and (114) reflexes of ferrite films textured with magnetic field perpendicular to film plane; ((0006), (10$\bar{1}$7) and (11$\bar{2}$4) reflexes in hexagonal indexing).

x = 0 to 7 kOe for x = 1; at about x = 1.7 the uniaxial anisotropy completely disappears.[9]

The microwave properties were measured in a waveguide arrangement. The variation of the reflection coefficients vs. frequency for the Ga-substituted ferrites is shown in Fig. 4. The resonant frequency slightly increases with Ga-concentration (Fig. 4, inset). In contrast, the FMR frequency of Sc-substituted ferrites significantly decreases with increasing x[11] (Fig. 4, inset). M-type Ba ferrite exhibits a resonance frequency of about 45-50 GHz. Ustinov *et al.*[21] report on the resonance frequency of single-crystalline Ba ferrite films; at zero applied field they report a f_r = 47 GHz. The slight increase of resonance frequency (Fig. 4) with x for Ga-substitution is consistent with fact that the anisotropy field is almost independent on x,[9] and the observation of a coercivity only slightly decreasing with Ga-content. Because of these findings, Ga-substituted Ba ferrite is not an appropriate material for microwave components designed for operating in the 30 GHz range. On the other hand, $BaSc_{0.5}Fe_{11.5}O_{19}$ has a resonance frequency of f_r = 30 GHz, and is a good candidate as self-biased microwave ferrite.

We studied the post-firing and co-firing behavior of ferrite thick film layers with composition $BaSc_{0.5}Fe_{11.5}O_{19}$ with LTCC tapes. Ferrite paste was printed onto the top surface of a fired CT708 LTCC multilayer substrate, dried in a magnetic field, and post-fired at 900 °C. The ferrite films exhibit a thickness of about 20 μm for a single printing cycle. The films show good adherence to the substrate (Fig. 5a). As alternative approach, we built up a multilayer stack of ferrite tapes sandwiched between LTCC tapes. After co-firing at 900 °C the multilayer stack was well sintered; no cracks, delamination or significant chemical interactions between the layers were observed (Fig. 5b). This is the first time, that post-firing of a layer of Sc-substituted Ba hexagonal ferrite onto LTCC and co-firing of ferrite and LTCC tapes has been demonstrated. To investigate the crystallographic orientation of the printed and post-fired ferrite thick film, we performed XRD texture characterization with an Eulerian cradle. As example, pole figures of (006), (107) and (114) reflections (or (0006), (10$\bar{1}$7) and (11$\bar{2}$4) peaks in hexagonal indexing) were determined (Fig. 6). Examination of the (006) pole figure reveals a strong texture of the sintered ferrite films thick film. The same conclusion results from (107) and (114) pole figures; the observed rings are also indicative of a fiber texture. These findings represent massive support for a strong preferential orientation of the ferrite particles in the film perpendicular to the film plane (⊥). This is an important prerequisite for the ability to self-biasing of these hexagonal ferrite layers.

IV. CONCLUSIONS

The phase formation behavior of Ga- and Y-substituted ferrites $BaMe_xFe_{12-x}O_{19}$ ($0 \le x \le 2$) was found to be quite different. Whereas Ga forms a complete solid solution within this compositional range, Y does not seem to not dissolve in the ferrite lattice at all. The formation of a Ga-substitution series is also indicated by the linear variation of lattice parameters with substitution rate (Vegard's law). The saturation magnetization of the Ga-substituted substituted ferrites decreases with increasing substitution rate x, similar to what is known for Sc-substituted ferrites. This might be caused by weakened exchange interactions due to substitution of non-magnetic ions for ferric ions. The coercivity, however, decreases moderately for Ga samples, whereas in the case of Sc-ferrites it significantly drops with x. This reflects a reduction of anisotropy field upon Sc-substitution. This is consistent with the observed slight increase of resonance frequency with Ga-substitution only. Sc-substitution, on the other hand, shifts the FMR to lower frequencies as consequence of the reduced magneto-crystalline anisotropy as compared to pure $BaFe_{12}O_{19}$. Oriented films of Sc-substituted ferrite on LTCC substrates were fabricated using screen-printing, drying in a magnetic field, and firing at 900 °C. Ferrite green tapes and LTCC tapes were successfully co-fired at 900 °C. These examples demonstrate that substituted Ba ferrite layers can be integrated in LTCC microwave modules.

ACKNOWLEDGMENTS

The authors acknowledge funding and support of the German Aerospace Center (DLR) on behalf of the German Federal Ministry of Economics and Technology (BMWi) under grant 50YB1720. The authors thank J. Schur (Technical University Ilmenau) for laser machining of samples and R. Müller (IPHT Jena) for help with VSM measurements.

REFERENCES

[1] M. Pardavi-Horvat, J. Magn. Magn. Mater. **215-216**, 171 (2000).
[2] Ü. Özgür, Y. Alivov, and H. Morkoc, J. Mater. Sci. Mater. Electron. **20**, 789 (2009).
[3] V. Harris, A. Geiler, Y. Chen, S. Yoon, M. Wu, A. Yang, Z. Chen, P. He, P. Parimi, X. Zuo, C. E. Patton, M. Abe, O. Archer, and C. Vittoria, J. Magn. Magn. Mater. **321**, 2035 (2009).
[4] V. Harris, Z. Chen, Y. Chen, S. Yoon, T. S. A. Geiler, A. Yang, Y. He, K. Ziemer, N. Sun, and C. Vittoria, J. Appl. Phys. **99**, 08M911 (2006).
[5] P. Shi, S. Yoon, X. Zuo, I. Kozulin, S. Oliver, and C. Vittoria, J. Appl. Phys. **87**, 4981 (2000).

[6]H. Kojima, in *Ferromagnetic Materials*, edited by E. P. Wohlfahrt (North-Holland Publ., Amsterdam, 1982), Vol. 3, p. 305.
[7]J. Smit, H. P. J. Wijn, and L. Ferrites, *Bibliothèque Technique Philips* (Dunod Paris, 1961).
[8]L. M. Silber, E. Tsantes, and P. Angelo, J. Appl. Phys. **38**, 5315 (1967).
[9]P. Röschmann, M. Lemke, W. Tolksdorf, and F. Welz, Mat. Res. Bull. **19**, 385 (1984).
[10]G. F. Dionne and J. F. Fitzgerald, J. Appl. Phys. **70**, 6140 (1991).
[11]S. Bierlich, F. Gellersen, A. Jacob, and J. Töpfer, Mat. Res. Bull. **86**, 19 (2017).
[12]A. D. Shchurova, T. M. Perekalina, and S. S. Fonton, Sov. Phys. JETP **31**, 840 (1970).
[13]S. V. Trukhanov, A. V. Trukhanov, V. G. Kostishyn, L. V. Panina, A. V. Trukhanov, V. A. Turchenko, D. I. Tishkevich, E. L. Trukhanova, V. V. Oleynik, O. S. Yakovenko, L. Y. Matzui, and D. A. Vinnik, J. Magn. Magn.Mater. **442**, 300 (2017).
[14]Y. Chen, Y. Wang, Y. Liu, Q. Liu, C. Wu, B. Qi, and H. Zhang, J.Mater. Sci. Mater. Electr. **30**, 5911 (2019).
[15]S. Bierlich, T. Reimann, F. Gellersen, A. F. Jacob, and J. Töpfer, J. Europ. Ceram. Soc. **39**, 3077 (2019).
[16]F. Bachmann, R. Hielscher, and H. Schaeben, Solid State Phenomena **160**, 63 (2010).
[17]R. D. Shannon, Acta Cryst. A **32**, 751 (1976).
[18]G. Albanese, A. Deriu, E. Lucchini, and G. Slokar, Appl. Phys. A **26**, 45 (1981).
[19]D. Seifert, J. Töpfer, F. Langenhorst, J.-M. Le Breton, H. Chiron, and L. Lechevallier, J. Magn. Magn. Mater. **321**, 4045 (2009).
[20]T. M. Clark, B. J. Evans, and G. K. Thompson, J. Appl. Phys. **85**, 5229 (1999).
[21]A. B. Ustinov, A. S. Tatarenko, G. Srinivasan, and A. M. Balbashov, J. Appl. Phys. **105**, 023908 (2009).